GEORG-AUGUST-UNIVERSITÄT
GÖTTINGEN

Fakultät für
Physik

Bachelor Thesis

Thresholds for the Onset of Convection and Nucleation in Phase Separation of a Binary Fluid

Übergänge zum Einsatz von Konvektion und Nukleation in der Phasenseparation eines binären Fluids

prepared by

Jan-Hendrik Trösemeier

from Stadtoldendorf

at the Max Planck Institute for Dynamics and Self-Organization

Thesis period:	15th October 2010 until 21st January 2011
First referee:	Prof. Dr. Jürgen Vollmer
Second referee:	Prof. Dr. Ulrich Parlitz

We investigate the phase separation of a binary fluid which is driven by a slow temperature ramp. Via a Galerkin approximation we explore the onset of convective and diffusive instabilities. We give explicit analytic expressions for the critical parameters and their onset. Beyond the threshold we identify a third class of solutions: oscillatory behaviour of composition which is also observed in experiments.

Contents

1 Introduction **1**
1.1 Motivation 1

2 Modelling a Binary Fluid **3**
2.1 Thermodynamics 3
2.2 Dimensionless Units 9

3 Slow Temperature Ramp **12**
3.1 The Stable Diffusion Profile 12
3.2 Stability Analysis 14

4 Fast Temperature Ramp **19**
4.1 Equations of Motion 19
4.2 A Three Mode Model 23
4.2.1 Equations and Linearization 23
4.2.2 Discussion of Solutions 24
4.3 The Five Mode Model 32

5 Discussion and Conclusion **38**
5.1 Summary 38
5.2 Discussion 38
5.3 Outlook 40

Acknowledgements **41**

Appendix **42**

A Phase Transitions **42**
A.1 Mean Field Approach 42

References **46**

1 Introduction

1.1 Motivation

The dynamics and behaviour of phase transitions is of longstanding interest for diverse areas of reasearch like the classical transitions in liquids and gases, superfluidity or liquid crystals and can even be applied in less obvious situations like for swarm behaviour of animals, rock formation in magma chambers and the dynamics of clouds. It all started when the first scientists noted the jump-like transitions between solid, gas and liquid phases. These could be well explained since the advent of rigorous thermodynamics. However, not all phase transitions appear as abrupt changes in the symmetries of the solutions of a system. Some even show exotic, or rather, unexpected behaviour. Of a special importance and an example of an unexpected transition is the λ-transition to superfluidic Helium. Here, the viscosity disappears completely while the thermal conductivity becomes infinite. This discovery led Ehrenfest to thoroughly classify phase transitions in the early 40s [4]. He proposed a model that distinguishes transitions by discontinuities of the thermodynamic response functions. Pioneering work in this regard was also performed by Landau who proposed a model for the free energy of a system that undergoes phase separation by focusing on the symmetries present. Of those, especially the Landau-ϕ^4 model was successfully applied to a broad case of phase separations [8]. In out later analysis we will turn to it to describe the thermodynamics and demixing properties of a binary liquid. Later, a major revision occurred with the appearance of field theories, as it became possible to describe the coupling of a scalar quantity to its surrounding in a consistent manner. This approach, also called the renormalization group approach, made it possible to study systems near their critical points. Additionally the introduction of Feynman's path integral formalism and Feynman graphs allowed for the analysis of order parameters and their scaling properties near regions of criticality (see e.g. [5]). From hereon Hohenberg and Halperin classified a large class of real world phase separating models according to conserved quantities, critical parameters and influence of noise [9]. Of special interest for our work is their classification of how a mixture of two fluids behaves near its critical point, i.e. the model H. It is commonly used for the analysis of systems that are rapidly quenched into demixing. In this work we will use it to describe the binary fluid model.
Our aim is to provide a model that describes a broad class of demixing fluids that undergo slow heating and give insight into the generic porperties of such a phase

separation.

We consider a binary mixture of two miscible fluids with different densities that undergo a slow ramp of temperature until they demix. We will only look at systems that are heated slowly and can be considered isothermal. This means there is no need to include the diffusion of temperature. Therefore, our system can be described as a simple diffusion in concentration advected by the hydrodynamics.

Since we will also assume that the fluid viscosities are the same, the demixing is initially driven by gravitational separation of coarsened phase structures due to density differences. It is supported by an external ramp rate of temperature. Additionally, there is also the inherent possibility to demix via spinodal decomposition or nucleation if the supersaturation becomes large. To model this behaviour we have to look at the equations governing fluid motion and advection-diffusion of the phase composition. To account for the demixing we use a mean-field model for the free energy. With this approach we can describe our system and make a stability analysis based on a Galerkin approximation for both, slowly and rapidly driven heating around the stable, diffusive solution of the governing equations of motion.

2 Modelling a Binary Fluid

2.1 Thermodynamics

We will first give a thermodynamic description of our model system, i.e., we will describe the time evolution of the phase composition. In a second step we will describe how this composition is then advected by the flow.
As our model we consider a fluid consisting of two phases in a box of side length Λ, which we will also refer to as a binary fluid. Additionally a slow heating rate to the system is applied in the sense that we can neglect the diffusion of temperature and also, by adiabatic elimination, any local fluctuations. This allows us to concentrate on the diffusion of composition ϕ only. For simplicity we furthermore assume that both phases occupy the same volume so that we only need to model one phase and know by symmetry the behaviour of the other.
To start the derivation of the equations of motion we look at the time dependence of the composition ϕ. A local change occurs because of a flux $\mathbf{j}_\phi$ via an continuity equation:

$$\frac{\mathrm{d}\phi}{\mathrm{d}t} = -\nabla \mathbf{j}_\phi. \tag{2.1}$$

This flux occurs because of a spatial difference in the chemical potential μ times some mobility constant M

$$\mathbf{j}_\phi = -M\nabla\mu. \tag{2.2}$$

The chemical potential on the other hand can be obtained by looking at the free energy F of the fluid. The composition will minimise this free energy if we let it go into equilibrium and can be obtained by the functional derivative

$$\mu = \frac{\delta F}{\delta \phi} \tag{2.3}$$

Here, the operator $\frac{\delta}{\delta\phi}$ is given as

$$\frac{\delta}{\delta\phi} = \frac{\partial}{\partial\phi} - \nabla\frac{\partial}{\partial(\nabla\phi)}. \tag{2.4}$$

In a continuum description of a scalar field that is coarse grained according to mean-field theory the free energy is a functional of the order parameter, i.e., in our case of the composition. A model satisfying the symmetry requirements of rotational

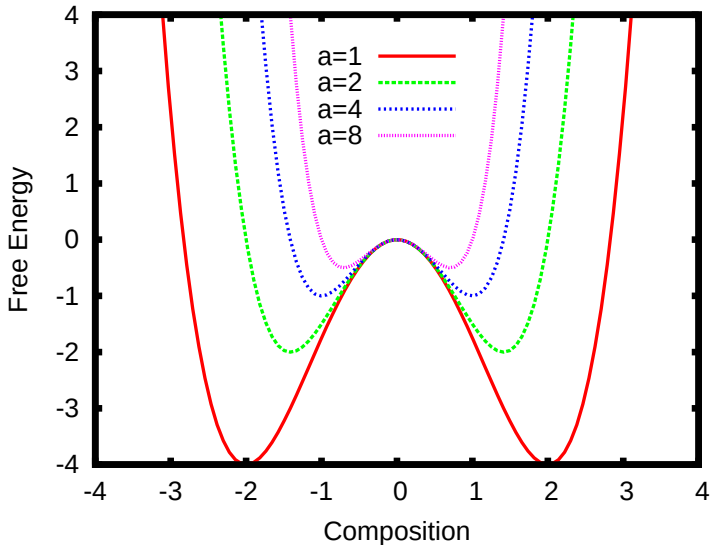

Figure 1: The free energy as a double well potential. It has two minima describing stable composition profiles at $\pm\sqrt{\frac{a}{b}}$ if a,$b > 0$. If a,$b \leq 0$ then the free energy is just a parabola with one minimum at 0 and no phase separation occurs. In this graph we chose $b = 2$ and $a = 1$,2,4,8 resulting in less distinctive minima if a increases.

invariance and the demand of being simple whilst simultaneously being capable of capturing the phase separation dynamics is the Landau free-energy

$$F[\phi(\mathbf{r},t)] = \int_V \mathrm{dV} \left[F_0[\phi(\mathbf{r},t) + \frac{K}{2}.(\nabla\phi(\mathbf{r},t))^2 \right], \tag{2.5}$$

where F_0 is a double-well potential and $\frac{K}{2}.(\nabla\phi(\mathbf{r},t))^2$ penalises steep gradients in compositions. This resembles interfacial or surface tension[1]. Usually the double well potential is chosen to have the order of 4 with constants a,b as

$$F_0[\phi] = \frac{1}{4}b\phi^4 - \frac{1}{2}a\phi^2. \tag{2.6}$$

This equation has the aforementioned form only if a,b are positive. Then it possesses a local minimum at $\phi = 0$ and two global minima at $\phi_0 = \pm\sqrt{\frac{a}{b}}$ which are the equilibrium values of ϕ (cf. Fig.1).

This double well potential gives rise to a phase diagram with simple miscibility gap shown in Fig. 2. Note, that in a phase diagram the stable composition ϕ_0 becomes

[1] A short revision of mean-field theory and the derivation of the ϕ^4 model is also included in the appendix A

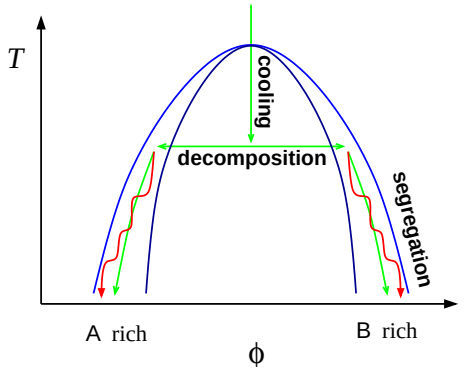

Figure 2: In this picture a simple miscibility gap for a symmetric binary fluid is shown. The spinodal is depicted as the inner dark-blue line and the binodal as the outer and light-blue line. In between the binodal and spinodal the system is metastable. If the binary fluid is cooled inside the gap along the green arrow the composition ϕ demixes into two coexisting phases with an equilibrium at $\pm\phi_0$ on the binodal. The new composition in the respective phases is indicated by the horizontal line. When the cooling is sustained the system again demixes and thereby follows the wavy, solid line while undergoing cyclic repetitions of demixing. [12]

a function of temperature with a spinodal where $\phi_0(T) \approx \alpha T^2 + \beta T^4$ and a binodal where $\phi_0(T)$ grows like a power law $\phi_0(T) \propto T^{\frac{1}{2}}$. For simplicity we will always assume that the critical point lies at $T_C = 0$. The stable composition is indicated by $\phi = \pm\phi_0(T)$ and does only depend on time via the temperature and not explicitly. If we now insert the chemical potential from Eqn. 2.4 into the diffusion equation Eqn. 2.3 we obtain

$$\frac{\mathrm{d}\phi}{\mathrm{d}t} = \nabla M \nabla \frac{\delta F}{\delta \phi}. \tag{2.7}$$

in the generic case and by eliminating one parameter b by the equilibrium value of composition ϕ_0 with replacing $b \to \frac{a}{\phi_0^2}$ for the Landau-free-energy

$$\begin{aligned} \frac{\mathrm{d}\phi}{\mathrm{d}t} &= \nabla M \nabla (b\phi^3 - a\phi - K\nabla^2\phi) \\ &= \nabla M a \phi_0 \nabla \left(\frac{\phi^3}{\phi_0^3} - \frac{\phi}{\phi_0} - \frac{K}{a}\nabla^2 \frac{\phi}{\phi_0} \right) \end{aligned} \tag{2.8}$$

This diffusion equation is also called the Cahn-Hilliard-Equation. Stable solutions of this equations have the form of bubbles or kink-antikink-pairs, i.e., a layering of stable phases (e.g. for phases A,B the layering would be ABAB and the thickness would correspond to a fraction of the system size). To get a feeling of how this

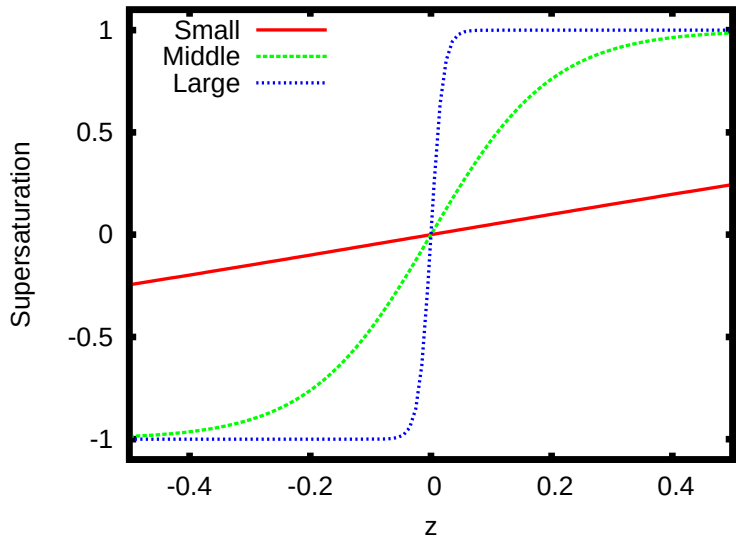

Figure 3: The stable solution plotted for $\sqrt{\frac{a}{K}} = \{1,10,100\}$. It starts of as a linear deviation and approaches a steep meniscus with decreasing K.

stable solutions look and how we should interpret K, we take the limit of small K and set the left hand side of Eqn. 2.7 equal to zero, consider the problem as homogeneous in y direction (where the meniscus forms at z=0) and imply no-flux boundary conditions at $z = \pm\infty$. Integrating once, we get the flow $\mathbf{j}_\phi$ which also has to vanish in equilibrium. And, by integrating a second time, we arrive at:

$$-\gamma = \left(\frac{\phi}{\phi_0} + \phi^3 - \frac{K}{a}\frac{\mathrm{d}^2}{\mathrm{d}z^2}\phi\right), \tag{2.9}$$

where $\gamma := (\frac{K}{a}\frac{\mathrm{d}^2}{\mathrm{d}z^2}\phi)$ at z=0. If we set $\gamma = 0$ and take the limit of $K \to 0$ this equation allows a very simple solution in the form of

$$\frac{\phi_S}{\phi_0} = \tanh\left(\sqrt{\frac{a}{K}}z\right). \tag{2.10}$$

It resembles two domains in which the composition takes on either of its equilibrium values and exhibits a sharp meniscus close to $z = 0$ (cf. Fig 3).

This also allows us to gain additional insight on how to interpret K:
If K decreases the region where most of the change near the meniscus decreases in width. If we therefore want to compute a characteristic interface width δ where p

percent of the change in composition occurs we can look at the equation

$$\int_{-\delta}^{\delta} \partial_z \tanh\left(\sqrt{\frac{a}{K}}z\right) \mathrm{d}z = p \tag{2.11}$$

and solve for δ. We obtain

$$\delta = \tanh^{-1}\left(\frac{p}{2}\right)\sqrt{\frac{K}{a}}. \tag{2.12}$$

We can now note that $\frac{K}{a}$ is proportional to the square of width δ^2.
Also, since the order parameter is conserved, phase separation in later times is mainly described by crossing of composition through the aforementioned interface. One way to look at the stable and long-term behaviour is by linearizing around the Cahn-Hilliard-Equation around the minimum at ϕ_0 and noting that ∇^4 - which scales as an inverse length scale $\frac{1}{\Lambda^4}$ - can be neglected. This leads to

$$\frac{\partial \phi}{\partial t} = Ma\left(\nabla^2 \phi\right). \tag{2.13}$$

This is just the limit of ordinary diffusion.
At this point, we could already start to look at the time evolution and evaluate the total derivative $\frac{\mathrm{d}}{\mathrm{d}t}$. However, if we first rewrite the diffusion equation 2.8 as

$$\frac{\dot{\phi}}{\phi_0} = \nabla Ma \nabla\left(\frac{\phi^3}{\phi_0^3} - \frac{\phi}{\phi_0} - \frac{K}{a}\nabla^2\frac{\phi}{\phi_0}\right) \tag{2.14}$$

it is compelling to introduce a new variable, the supersaturation φ, such that

$$\varphi = \frac{\phi}{\phi_0}. \tag{2.15}$$

This is important since the equilibrium composition ϕ_0 is a function of temperature and thus depends on time if a heating rate is applied. With this substitution the time dependency of the coefficients in the transport equation is absorbed into φ. We can now work out the rhs of Eqn.2.14. We have to include that the composition gets advected by the velocity field $\mathbf{u}$ of the fluid's flow. This leads to an additional

advective derivative such that

$$\begin{aligned}\frac{1}{\phi_0}\frac{\mathrm{d}\phi}{\mathrm{d}t} &= \frac{1}{\phi_0}\frac{\mathrm{d}}{\mathrm{d}t}(\varphi\phi_0)\\ &= \xi(t)\varphi + \frac{\mathrm{d}\varphi}{\mathrm{d}t}\end{aligned}$$

with a heating rate

$$\xi(t) = \frac{1}{\phi_0}\frac{\mathrm{d}\phi_0}{\mathrm{d}t}. \tag{2.16}$$

This $\xi(t)$ depends on time via

$$\xi(t) = \frac{1}{\phi_0}\left(\frac{\partial\phi_0}{\partial t} + \frac{\partial\phi_0}{\partial T}\frac{\partial T}{\partial t}\right)$$

and becomes negligible if we, for example, choose a constant heating rate $\partial_t T = \text{const.}$, since $\partial_T\phi_0$ grows fast. To observe the system for an extended period of time at similar amplitudes of φ we instead want to have a driving rate which is constant. Therefore we choose our heating rate ξ to be

$$\xi = \frac{1}{\phi_0}\frac{\mathrm{d}\phi_0}{\mathrm{d}t} = \text{const.} \tag{2.17}$$

When the width of the two-phase region grows like a power law $\phi_0 = \left(\frac{T-T_c}{T_c}\right)$ the appropriate temperature profile, i.e., one that amounts to a constant ξ takes the form

$$T(t) = T_c + \left(\frac{c}{A}\right)^{\frac{1}{\alpha}} e^{\frac{\xi}{\alpha}t}, \tag{2.18}$$

which was used by Auernhammer and Vollmer successfully in experiments [2].
If we now define a diffusion constand D that we assume to be independent of position by

$$D = 2Ma \tag{2.19}$$

we obtain a diffusion equation in supersaturation

$$\frac{\partial\varphi}{\partial t} + (\mathbf{u}\nabla)\varphi = \nabla D\frac{3\varphi - 1}{2}\nabla\varphi + \frac{DK}{a}\nabla^4\varphi. \tag{2.20}$$

For the description of how the composition is advected we also have to describe how to evolve the flow. Hohenberg classified dynamical models treated with renormalisation-group methods of mean field theory according to universal

properties[9]. These properties are the dimension of the order parameter, the conserved quantities and constants of motion. His classification ranges from the Ising model to Heisenberg antiferromagnets and luckily also includes the critical behaviour of binary fluids, referred to as model H. In this model the composition as well as the fluid volume are conserved quantities, that means, there is a continuity equation described by the fluids flow $\mathbf{u}$ and the diffusion current $\mathbf{j}$. The time evolution in this model is described by the Navier-Stokes-Equations and the diffusion equation, where the sound modes are ignored and the pressure acting on the fluid assumed to be constant. In this case we get with $\alpha = \frac{1}{\rho}\mathrm{d}\rho\mathrm{d}\phi$

$$\frac{\partial \mathbf{u}}{\partial t} + \mathbf{u}.\nabla\mathbf{u} = \nu\nabla^2\mathbf{u} + \alpha g\phi\mathbf{e}_z - \frac{1}{\rho}\nabla p - \frac{K}{\rho}\nabla^2\phi\nabla\phi. \tag{2.21}$$

The buoyancy term $\alpha g\phi\mathbf{e}_z$ arises from the Boussinesq approximation of gravity $f_g = \rho g \approx g\Delta\rho$ which is valid if the difference in density of the two phases $\Delta\rho$ is small compared to the background density of the respective fluids. The term accounting for surface tension $-K\nabla^2\phi\nabla\phi$ derives from the transport of a fluid volume $\phi\delta\mu$ over the chemical potential difference $\delta\mu$. Altogether, this leads to a driving force of $\phi\nabla\mu$ and

$$\phi\nabla\mu = \phi\frac{\delta F}{\delta\phi} = \phi\frac{\delta^2 F}{\delta\phi^2}\nabla\phi = K\nabla^2\phi\nabla\phi. \tag{2.22}$$

2.2 Dimensionless Units

We can now combine the Navier-Stokes and diffusion equation. To give it a suitable form for further analysis, we nondimenzionalize the equations

$$\frac{\partial \mathbf{u}}{\partial t} + \mathbf{u}.\nabla\mathbf{u} = \nu\nabla^2\mathbf{u} + \alpha g\phi\mathbf{e}_z - \frac{1}{\rho}\nabla p - \frac{K}{\rho}\nabla^2\phi\nabla\phi \tag{2.23}$$

and

$$\frac{\mathrm{d}\varphi}{\mathrm{d}t} = \frac{1}{\phi_0^2}\nabla.M\nabla\frac{\delta^2 F}{\delta\varphi^2}\nabla\varphi \tag{2.24}$$

$$= \nabla 2Ma\left[\frac{3\varphi^2 - 1}{2} + \frac{K}{a}\nabla^3\varphi\right]\nabla\varphi \tag{2.25}$$

Choosing the following units for length, time and mass

$$\mathbf{r} = \Lambda \mathbf{r}^* \tag{2.26}$$

$$t = \frac{\Lambda^2}{D} t^* \tag{2.27}$$

$$m = \rho \Lambda^3 m^* \tag{2.28}$$

and defining

$$N_0 = \frac{\alpha g \phi_0 \Lambda^3}{D\nu}, \tag{2.29}$$

$$N_1 = \frac{\nu}{D}, \tag{2.30}$$

$$N_2 = \frac{\xi \Lambda^2}{D}, \tag{2.31}$$

$$S = \frac{K\phi_0^2}{\rho \Lambda^3} \tag{2.32}$$

$$M = \frac{K}{a\Lambda^2}. \tag{2.33}$$

we can nondimensionalize both equations of motion:

$$\frac{\partial \mathbf{u}}{\partial t} + \mathbf{u}.\nabla \mathbf{u} = N_1[\nabla^2 \mathbf{u} + N_0 \varphi \mathbf{e}_z - \nabla p - S\nabla^2 \varphi \nabla \varphi] \tag{2.34}$$

$$\frac{\partial \varphi}{\partial t} + \mathbf{u}.\nabla \varphi = \nabla.[f(\varphi)\nabla \varphi] - N_2 \varphi - M\nabla^4 \varphi, \tag{2.35}$$

In these equations the constants appear in the following way: N_0 is interpreted as corresponding to the strength of gravity acting on a fluid volume, N_1 as some material constant also known as Schmidt number, and N_2 as a heating rate applied to the system. The additional constants S and M both define how surface tension acts on a fluid volume and on composition

A peculiar point in this nondimensionalization is the following: Since the heating rate ξ is kept constant Eqn. 2.17 dictates that ϕ_0 is a function of time, i.e., $\phi_0(t) = \phi_0(t=0)e^{\xi t}$ and thus N_0 is not a constant, but does depend on time explicitly. In dimensionless units we have

$$\phi_0(t) = \phi_0(t=0)e^{N_2 t}. \tag{2.36}$$

This, though, does not play a large role for the stability thresholds discussed in this work since for the onset of convectional instabilities we can consider small values of t so that $N_2 t$ stays small and $e^{N_2 t} \approx 1$.
In the subsequent two sections of this work we will show how these equations lead to diffusive and convective instabilities in the binary fluid.

3 Slow Temperature Ramp

3.1 The Stable Diffusion Profile

First we look at a slowly driven system with small N_2 and use a stability analysis around the stable diffusive solution[2]. In this case the time derivatives as well as the fluid velocity vanish. Therefore, we have

$$\frac{\partial \varphi}{\partial t} = 0 \quad \text{and} \quad \mathbf{u} = 0. \tag{3.1}$$

We also assume the solutions to be homogeneous in horizontal direction, such that we may only regard the two dimensional case without neglecting a substantial part of physics. This leads to a simplified version of Eqns. 2.34 and 2.35

$$N_0 \varphi_0 \mathbf{e}_z - \partial_z p_0 = 0 \tag{3.2}$$

$$\partial_z [f(\varphi_0) \partial_z \varphi_0] - N_2 \varphi_0 = 0, \tag{3.3}$$

with $f(\varphi) = \frac{3\varphi^2 - 1}{2}$. We can further simplify this due to the fact that f varies slowly with φ. For slow heating, i.e., $N_2 < N_{2,cr}$ we may use the approximation

$$f(\varphi_0(0)) = 1. \tag{3.4}$$

In first order we arrive at an ordinary differential equation for the saturation profile

$$(\partial_z^2 - N_2)\varphi_0 = 0 \tag{3.5}$$

The solution of this ODE depends on our boundary conditions. Since we do not have interfacial effects these are

$$\varphi_0(z = 0) = 1 \tag{3.6}$$

[2] Using dimensional analysis we can get an estimate on how small a critical value of N_2 should be and what velocity scale of the ramping we may consider as slow. In the paper [12] it was shown that the velocity scale $\hat{v} = \partial_t T = N_{2,cr} \left(\frac{\Lambda^2}{D} \partial_T \frac{1}{\phi_0} \right)^{-1}$ takes values in the order of K/h [12] near a critical value of N_2 for a system size in the order of a few cm and also that $N_{2,cr} \approx \mathfrak{O}(1)$.

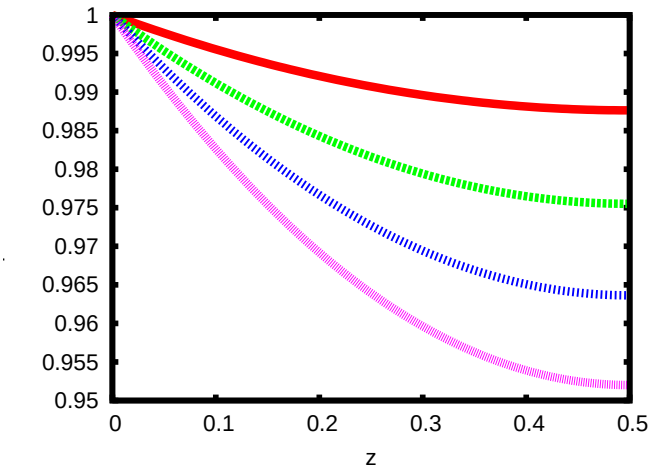

Figure 4: The stable supersaturation profile for different values of N_2. The graph is displayed for ($x \in [0,0.5]$) and $N_2 = 0.1,0.2,0.4,0.5$ and has to be continued anti-symmetrically in negative z-direction. The system is in equilibrium at the meniscus, where z=0 (This is actually enforced by the choice of our boundary conditions). The solution deviates more from the stable profile if the heating rate N_2 increases. Also it can be seen that the slope at $z = \frac{1}{2}$ equals zero, since there is no flux through the walls of the container.

at the phase boundary, where the phase composition takes its equilibrium value and

$$\frac{\partial \varphi_0}{\partial z}\left(z = \frac{1}{2}\right) = 0 \tag{3.7}$$

at the system's physical boundaries since there is no flux through the surrounding box. This leads to a solution (cf. Fig 4)

$$\varphi_0 = \frac{\cosh\left[\sqrt{N_2}(z - \frac{1}{2})\right]}{\cosh\left[\frac{\sqrt{N_2}}{2}\right]} \tag{3.8}$$

that describes the stable diffusive profile of the supersaturation. It has to be continued anti-symmetrically to obtain the profile for negative values of z.

3.2 Stability Analysis

To analyse when instabilities kick in we vary the stable profile with small variations

$$\mathbf{u} = \delta\mathbf{u}(\mathbf{r},\mathbf{t}) \tag{3.9}$$

$$\varphi = \varphi_0(z) + \delta\varphi(\mathbf{r},t) \tag{3.10}$$

$$p = p_0(z) + \delta p(\mathbf{r},t). \tag{3.11}$$

Furthermore, we consider all variations of second order, e.g., $\delta\varphi\delta\mathbf{u}$ as small and neglect them. Inserting these into our equations of motion 2.34 and 2.35 for $f(\varphi) = 1$ and no surface tension we get

$$\frac{\partial\delta\mathbf{u}}{\partial t} = N_1\left[\nabla^2\delta\mathbf{u} + N_0(\delta\varphi)\mathbf{e}_z - \nabla(\delta p)\right] \tag{3.12}$$

$$\frac{\partial\delta\varphi}{\partial t} + \delta\mathbf{u}.\nabla\varphi_0 = \nabla^2\delta\varphi - N_2(\delta\varphi). \tag{3.13}$$

These equations can further be simplified with taking the double curl $\nabla\times\nabla\times$ of Eqn. 3.12

$$\frac{\partial\nabla^2\delta\mathbf{u}}{\partial t} = N_1\left[\nabla^4\delta\mathbf{u} + N_0\left(\nabla\partial_z - \mathbf{e}_z\nabla^2\right)(\delta\varphi)\right] \tag{3.14}$$

$$\frac{\partial\delta\varphi}{\partial t} = -\frac{\partial\varphi_0}{\partial z}\mathbf{e}_z.\delta\mathbf{u} + \left(\nabla^2 - N_2\right)(\delta\varphi). \tag{3.15}$$

To continue the analysis we make an ansatz of a planar wave in horizontal x direction with a complex time dependence for the variations

$$\begin{pmatrix}\delta\mathbf{u}(t)\\ \delta\varphi(t)\end{pmatrix} = \mathrm{e}^{\gamma t}\mathrm{e}^{ikx}\begin{pmatrix}\delta\mathbf{u}\\ \delta\varphi\end{pmatrix}. \tag{3.16}$$

Plugging this into Eqns. 3.14 and 3.15 and using the cylindrical symmetry of the setting we can sort the equation according to the order of derivatives in z-direction:

$$\left[-\partial_z^4 + \left(\frac{\gamma}{N_1} + 2k^2\right)\partial_z^2 - \frac{\gamma}{N_1}k^2 - k^4\right]\delta\mathbf{u} = N_0\begin{pmatrix}ik\partial_z\\ 0\\ k^2\end{pmatrix}(\delta\varphi) \tag{3.17}$$

$$\left[\partial_z^2 - k^2 - N_2 - \gamma\right](\delta\varphi) = \partial_z\varphi_0\mathbf{e}_z.\delta\mathbf{u}. \tag{3.18}$$

Thanks to the symmetry we may retrieve the whole velocity profile $\mathbf{u}$ solely from its z component w allowing us to combine the above equations into a single 6th order ODE by multiplying Eqn. 3.18 with $N_0 k^2$ and inserting it into Eqn. 3.17

$$\left[\partial_z^2 - k^2 - N_2 - \gamma\right]\left[-\partial_z^4 + \left(\frac{\gamma}{N_1} + 2k^2\right)\partial_z^2 - \frac{\gamma k^2}{N_1} - k^4\right] w = N_0 k^2 (\partial_z \varphi_0) w \tag{3.19}$$

In order to continue our stability analysis we expand the saturation $\partial_z \varphi_0$ and velocity profile w in Fourier series that satisfy the no-flux boundary conditions and that the solution is asymmetric at $z = 0$

$$\varphi = \sum_{k=-\infty}^{\infty} \varphi_k \sin(2k\pi z) \tag{3.20}$$

$$\tag{3.21}$$

This choice of summation from $-\infty$ to ∞ facilitates the shifting of indices, since we do not have to worry about the summation boundaries.
The Fourier expansion of the stable profile satisfies

$$N_0 \frac{\partial \varphi_0}{\partial z} = a_m \cos(2\pi m z) \tag{3.22}$$

where

$$\frac{\partial \varphi_0}{\partial z} = \frac{\sqrt{N_2}}{\cosh\left(\frac{\sqrt{N_2}}{2}\right)} \sinh\left[\sqrt{N_2}\left(z - \frac{1}{2}\right)\right] \tag{3.23}$$

and therefore

$$a_m = -\frac{2N_2 N_0}{N_2 + (2\pi m)^2}\left[1 - \frac{(-1)^m}{\cosh\left(\frac{\sqrt{N_2}}{2}\right)}\right] \tag{3.24}$$

Inserting the expansion into the equations of motions we arrive at

$$N_0 \partial_z \varphi_0 = -2N_0 N_2 \sum_{n=-\infty}^{\infty}\left(1 - \frac{(-1)^n}{\cosh\left(\frac{\sqrt{N_2}}{2}\right)}\right)\frac{\cos(2\pi n z)}{N_2 + (2\pi n)^2} \tag{3.25}$$

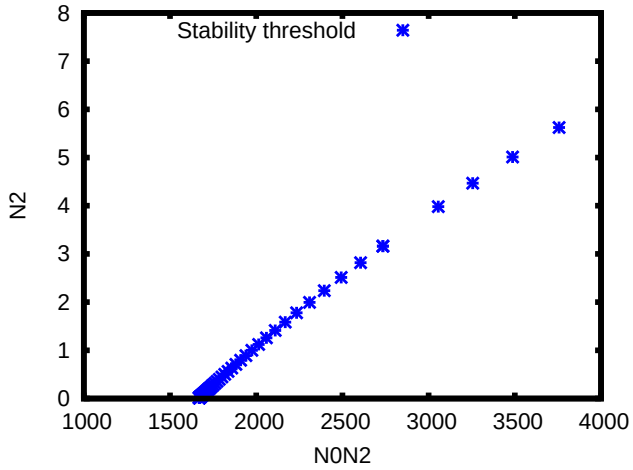

Figure 5: Onset of instabilities where N_2 is plotted linearily over N_0N_2. The points constitute a nearly linear slope and separate the stable region at the left from the convective unstable region to the right.

so that Eqn 3.19 becomes

$$N_0k^2\frac{\partial\varphi_0}{\partial z}w = -8\pi^2N_0N_2k^2\sum_{l=\infty}^{\infty}\sin(2\pi lz)\sum_{m=\infty}^{\infty}lm\frac{1-\frac{(-1)^{l-m}}{\cosh\left[\sqrt{N_2}/2\right]}}{[N_2+(2\pi)^2(l^2+m^2)]^2-64\pi^4l^2m^2}w_m. \tag{3.26}$$

The system becomes unstable if small variations are no longer damped ($\gamma > 0$), i.e., the bifurcation occurs at the smallest N_2 that admits a solution with ($\gamma = 0$). Inserting $\gamma = 0$ and rewriting the equation in matrix form $T_{lm}w_l = 0$ with

$$\begin{aligned}T_{lm} =&\frac{4kN_0\pi^2\left(1-(-1)^{l-m}\mathrm{sech}\left[\sqrt{N_2}\right]\right)lm}{\left(\pi^2\left(l^2+m^2\right)+N_2\right)^2-4l^2m^2\pi^4}-\\&\left[-(\pi l)^6-(3k^2+N_2)(\pi l)^4+(-k^4+(N_2+k^2)2k^2)(\pi l)^2-(N_2+k^2)k^4\right]\delta_{\mathrm{lm}}\end{aligned} \tag{3.27}$$

The non-trivial solutions of this system obey

$$\det(T) = 0. \tag{3.28}$$

Solving this equation for different modes gives us the result shown in Figs. 5, 6 and 7. Note that the onset of instabilities is independent of the parameter N_1, which describes the material properties of the mixture. We will show later on that this is indeed a generic property of such systems.

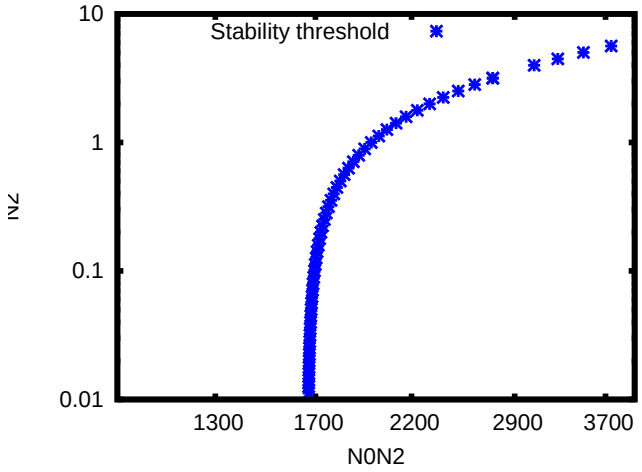

Figure 6: Double logarithmic graph of N_2 over N_0N_2. The left side constitutes a stable diffusive solution whereas the side right to the finger is unstable. In the case of small N_2 the graph approaches the critical number of $N_0N_2 = 1670$ asymptotically.

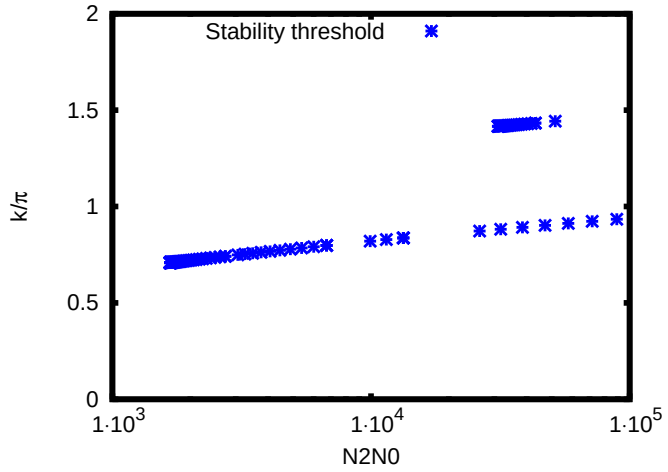

Figure 7: Plot of the wave-number $\frac{k}{\pi}$ (the additional factor of $\frac{1}{\pi}$ results from our e^{ikx} ansatz to accommodate the actual system size) vs. $\log(N_0N_2)$. Apparently the onset of convection is due to convection rolls with the aspect ratio slightly smaller than $\frac{k}{\pi} = 1$ at smallest N_0N_2. This is just what is expected for the onset of convection and resembles large, elliptic convection cells. At roughly $N_0N_2 = 2 \cdot 10^4$ new modes come into existence. These are not circular, but tend to become more elliptic if N_0 increases.

Furthermore, we can obtain the minimum value at which the system becomes unstable:

$$(N_0 N_2)_{Cr} \approx 1670. \tag{3.29}$$

This number coincides neatly with that obtained in the Rayleigh-Benard problem in which we have for convection near a free wall

$$Ra = \frac{g\beta}{\nu\bar{\alpha}}\Delta T \Lambda^3, \tag{3.30}$$

where β is the thermal expansion coefficient and $\bar{\alpha}$ is the thermal diffusivity. Now if we want to compare the Rayleigh number to our system we have to identify the corresponding terms in

$$N_0 N_2 = \frac{\alpha g \phi_0 \Lambda^5}{D^2 \nu}\xi. \tag{3.31}$$

The strength of gravity βg corresponds to $\alpha g \phi_0$, the thermal diffusivity $\bar{\alpha}$ to the diffusion constant D and the maximal temperature difference ΔT is equal to $\xi\Lambda^2$. Therefore it is reasonable to assume that $N_0 N_2 \approx Ra$.
Now the approximation is remarkably close since we have

$$Ra_c \approx 1700 \approx (N_0 N_2)_{Cr} \approx 1670 \tag{3.32}$$

as a critical Rayleigh number that describes the onset of convection rolls in this setup.
With this results we can determine the onset of convection cells if $N_2 < N_{2,cr}$, i.e., we pinpointed the threshold where the system loses stability against the first convection if the system is still diffusively stable. We can add this piece to a phase diagram of instabilities and will now consider faster heating rates to determine the onset of diffusive instabilities and to see what happens if both instabilities are present.

4 Fast Temperature Ramp

4.1 Equations of Motion

We now want to look at a system where the heating rate ξ is not nearly negligible and the assumption $f(\varphi) = 1$ remains no longer valid. We start with the Navier-Stokes-Equation 2.34 and the advection-diffusion equation 2.35 where we again dropped the term responsible for surface tension

$$\frac{\partial \varphi}{\partial t} + \mathbf{u}.\nabla\varphi = \nabla.[f(\varphi)\nabla\varphi] - N_2\varphi \tag{4.1}$$

with $f(\varphi) = \frac{3\varphi^2-1}{2}$. We again assume that gravity acts in z direction and that the convection rolls are oriented along the y axis allowing. Consequently we focus our attention on the spatial coordinates x,z and the time dependence.
To simplify the Navier-Stokes-Equation we introduce a stream function $\mathbf{\Psi}$ defined by

$$\mathbf{u} = \nabla \times \mathbf{\Psi} \tag{4.2}$$

For a flow in the (x,z)-plane $\mathbf{\Psi}$ has a very simple form,

$$\mathbf{\Psi} = \begin{pmatrix} 0 \\ \psi \\ 0 \end{pmatrix} \tag{4.3}$$

such that

$$u_x = -\partial_z \psi \tag{4.4}$$

$$u_z = \partial_x \psi \tag{4.5}$$

Inserting this into the equations of motion and taking the curl we arrive at

$$(\partial_t + (\partial_x\psi)\partial_z - (\partial_z\psi)\partial_x - N_1\nabla^2)\nabla^2\psi = N_1 N_0 \partial_x \varphi \mathbf{e}_z \tag{4.6}$$

$$(\partial_t + N_2 + (\partial_x\psi)\partial_z - (\partial_z\psi)\partial_x)\varphi = \nabla.\left(\frac{3\varphi^2-1}{2}\nabla\varphi\right). \tag{4.7}$$

We can use a Galerkin approximation to solve the equation. In practise this means we have to expand φ in a series and truncate it at a suitable order that still captures the part of physics we want to look at. Since we can assume that the fluid will behave

symmetrically around the interface, it is practical to exploit this in the choice of basis for our expansion. We therefore choose the Fourier expansion. This will allow us to transform the partial differential equations into a system of ordinary differential equations, since the differential operators correspond to multiplications in Fourier space. There are two possibilities of continuing from here on. Either we substitute $\mathbf{e}_z$ by a Heaviside functional $\Theta(z)$ to introduce a simple model for simulating a smooth phase boundary or we use the ansatz of an asymmetric φ around the interface. A problem in the first strategy is that the step function is not continuous at $z = 0$ and the Fourier expansion at such a place does not converges uniformly. Especially the Gibbs phenomenon will produce unphysical behaviour near the meniscus. We will hence concentrate on the phase field approach and use the stationary diffusive solution. Our aim is to expand the supersaturation and the stream function in a Fourier series. A suitable choice for the calculations ahead is

$$\varphi = \sum_{k=\infty}^{\infty} \sum_{l=-\infty}^{\infty} \varphi_{kl} e^{i\pi(kz+lx)} \tag{4.8}$$

$$\psi = \sum_{k=\infty}^{\infty} \sum_{l=-\infty}^{\infty} \psi_{kl} e^{i\pi(kz+lx)}, \tag{4.9}$$

since convolution becomes notably easier if no trigonometric identities need to be used and no care has to be taken for the domain of summation [3].
Additionally, we can exploit the symmetries inherent to our system to get rid of some of the modes. After all, φ has to be asymmetric around the interface at $z = 0$ (and therefore expanded in sin functions) and needs to posses a maximum at the boundary (because of the no-flux boundary conditions). Therefore only φ_{kl} modes with odd indices k have non-zero amplitudes. In the case of ψ, there is only the restriction that there is no flow through the boundaries of the container and no global rotation. We therefore place the origin of our coordinate system such that we have

$$\psi = \sin(\pi k z) \sin(\pi k x) \tag{4.10}$$

with odd modes in l and even modes in k. Then the coefficients ψ_{kl} will be real for all modes. This dictates

$$\phi = \sin(\pi k z) \cos(\pi l x), \tag{4.11}$$

[3] From here on we will use the Einstein-summation-convention so that $\varphi_{kl} \sin(kx) = \sum_{k=-\infty}^{\infty} \varphi_{kl} \sin(kx)$

where k is always odd and l always odd but for the first, zeroth mode $l = 0$. Thus the amplitudes φ_{kl} are imaginary for all modes.
We start with the Navier-Stokes Equation 4.6. The first term becomes

$$\partial_t \nabla^2 \psi_{kl} = -\pi^2 (k^2 + l^2) \dot{\psi}_{kl},$$

the second after substituting $(k + m \to k, l + n \to l)$[4] [5]

$$\begin{aligned}(\partial_x \psi)\partial_z \nabla^2 \psi &= kn(k^2 + l^2)\pi^4 \psi_{kl}\psi_{mn} \\ &= (k - m)n((k - m)^2 + (l - n)^2)\pi^4 \psi_{(k-m)(l-n)}\psi_{mn},\end{aligned}$$

the third with the same method

$$-(\partial_z \psi)\partial_x \nabla^2 \psi = -m(l - n)((k - m)^2 + (l - n)^2)\pi^4 \psi_{(k-m)(l-n)}\psi_{mn},$$

and finally

$$-N_1 \nabla^4 \psi = -(k^2 + l^2)^2 \pi^4 \psi.$$

Moreover, fot the RHS we obtain

$$N_1 N_0 \partial_x \varphi = i N_1 N_0 \pi l \varphi$$

Here, one eventually has to adjust the direction of gravity in every second copy of the system in order to make sure that supersaturation leads to density inversion in each copy of the system. To this end we multiply N_0 by a square-wave so that it is symmetric with respect to $z = 0$ and has a period of 2. This yields

$$\begin{aligned}-\pi^2(k^2 + l^2)\dot{\psi}_{kl} + (m - k)l((m - k)^2 + (n - l)^2)\pi^4 \psi_{(m-k)(n-l)}\psi_{kl} \\ -k(n - l)((m - k)^2 + (n - l)^2)\pi^4 \psi_{(m-k)(n-l)}\psi_{kl} \\ -(k^2 + l^2)^2 \pi^4 \psi_{kl} = -N_1 N_0 \pi l \frac{2}{2n + 1} \varphi_{(k-2n-1)l}.\end{aligned} \tag{4.12}$$

[4] For $\varphi \cdot \varphi$ can be easily described as a discrete convolution in Fourier space, where $\varphi \cdot \varphi = \varphi_{kl}\varphi_{mn} \exp\{-i\pi[(k + m)z + (l + n)x]\} = \varphi_{(k-m)(n-l)}\varphi_{mn} \exp\{-i\pi[(k + m]z + (l + n)x]\} = \varphi(k,l) * \varphi(m,n) = \varphi(k - m, l - n)\varphi(m,n)$

[5] Caveat: We implicitly assume that the derivative and the series expansion $\partial \sum_{-\infty}^{\infty} = \sum_{-\infty}^{\infty} \partial$ commutes. Though this is true for finite sums, we need uniform convergence in the relevant functions and their derivatives if the sum is an infinite series. However this Galerkin method provides good results nonetheless when we are careful with pathological functions.

We now turn to the diffusion Equation 4.7 in which we have

$$(\partial_t + N_2)\varphi = N_2\varphi + \dot{\varphi}$$

as well as

$$(\partial_x\psi)\partial_z\varphi = -(k-m)n\pi^2\psi_{mn}\varphi_{(k-m)(l-n)}$$

and

$$-(\partial_z\psi)\partial_x\varphi = m(l-n)\pi^2\psi_{mn}\varphi_{(k-m)(l-n)}.$$

Moreover, for the cubic nonlinearity we obtain

$$\begin{aligned}
\nabla\left(\frac{3\varphi^2-1}{2}\nabla\varphi\right) &= \frac{3}{2}\partial_x(\varphi^2\partial_x\varphi) - \frac{1}{2}\partial_x^2\varphi + \frac{3}{2}\partial_z(\varphi^2\partial_z\varphi) - \frac{1}{2}\partial_z^2\varphi \\
&= 3\varphi(\partial_x\varphi)^2 + \frac{3}{2}\varphi^2\partial_x^2\varphi - \frac{1}{2}\partial_x^2\varphi + 3\varphi(\partial_z\varphi)^2 + \frac{3}{2}\varphi^2\partial_z^2\varphi - \frac{1}{2}\partial_z^2\varphi \\
&= (-3\pi^2 nq - \frac{3}{2}\pi^2 q^2)\varphi_{(k-p-m)(l-n-q)}\varphi_{mn}\varphi_{pq} + \pi^2(l)^2\varphi_{kl} + \\
&\quad (-3\pi^2 mp - \frac{3}{2}\pi^2 p^2)\varphi_{(k-p-m)(l-n-q)}\varphi_{mn}\varphi_{pq} + \pi^2(k)^2\varphi_{kl}.
\end{aligned}$$

This leads eventually to the Galerkin representation

$$\begin{aligned}
&\dot{\varphi}_{kl} + N_2\varphi_{kl} + \pi^2(m(l-n) - (k-m)n)\psi_{mn}\varphi_{(k-m)(l-n)} \\
&= -\pi^2\left[3(nq+mp) + \frac{3}{2}(p^2+q^2)\right]\varphi_{(k-p-m)(l-n-q)}\varphi_{mn}\varphi_{pq} + \\
&\qquad \frac{1}{2}\pi^2\left[l^2+k^2\right]\varphi_{kl}.
\end{aligned} \tag{4.13}$$

The full system of equations can at best be handled in an approximation. To gain insight in the dynamics we rather concentrate on a heavily truncated system of equations that we can explicitly solve for the stationary modes of composition and velocity.

4.2 A Three Mode Model

4.2.1 Equations and Linearization

To begin our analysis of the discretized system of equations we first look at a minimal set of modes. An initial approach is to choose the minimal modes analog to the important ones for Rayleigh convection. This means we take the φ_{10} mode into account to describe the vertical deviation from the stable solution, the φ_{11} as the horizontal deviation and the ψ_{21} stream mode which describes a simple fluid motion in terms of the first convection mode . For this approach we get the following system of equations:

$$\frac{\mathrm{d}\varphi_{10}}{\mathrm{d}t} = -\varphi_{10}N_2 + \varphi_{10}\pi^2 + 4\psi_{21}\varphi_{10}\pi^2 - \frac{3}{2}\varphi_{10}^3\pi^2 + 9\varphi_{10}\varphi_{11}^2\pi^2 \tag{4.14}$$

$$\frac{\mathrm{d}\varphi_{11}}{\mathrm{d}t} = -\varphi_{11}N_2 + 2\varphi_{11}\pi^2 + 4\psi_{21}\varphi_{11}\pi^2 - 9\varphi_{10}^2\varphi_{11}\pi^2 + 9\varphi_{11}^3\pi^2 \tag{4.15}$$

$$\frac{\mathrm{d}\psi_{21}}{\mathrm{d}t} = \frac{4}{15}N_0N_1\varphi_{11} - 5N_1\pi^3\psi_{21}. \tag{4.16}$$

To analyse this system we linearize it and follow the stable solutions in dependence of the parameters N_0 and N_1[6]. Subsequently, we linearize the system around the stable solutions to be able to decide what kind of stability or bifurcations occur. We choose

$$\varphi_{10} = \bar{\varphi}_{10} + \delta\varphi_{10} \tag{4.17}$$

$$\varphi_{11} = \bar{\varphi}_{11} + \delta\varphi_{11} \tag{4.18}$$

$$\psi_{21} = \bar{\psi}_{21} + \delta\psi_{21}, \tag{4.19}$$

and define

$$\boldsymbol{\delta} = \begin{pmatrix} \delta\varphi_{10} \\ \delta\varphi_{11} \\ \delta\psi_{21} \end{pmatrix}, \tag{4.20}$$

[6]The stable solutions can be obtained by looking at the intersection of the φ_{10}, φ_{11} and ψ_{21} nullclines, i.e., by letting all time derivatives vanish.

so that we can write the linearized system as

$$\boldsymbol{\delta} = A\boldsymbol{\delta} + \mathbf{b}. \tag{4.21}$$

Here

$$\mathbf{b} = \begin{pmatrix} -\frac{N_2}{\pi^2}\bar{\varphi}_{10} + \bar{\varphi}_{10} - \frac{3}{2}\bar{\varphi}_{10}^3 + 9\bar{\varphi}_{10}\bar{\varphi}_{11}^2 + \frac{3}{2}\bar{\varphi}_{10}^2\bar{\varphi}_{30} - 3\bar{\varphi}_{10}\bar{\varphi}_{30}^2 + 4\bar{\varphi}_{10}\bar{\psi}_{21} \\ -\frac{N_2}{\pi^2}\bar{\varphi}_{11} + 2\bar{\varphi}_{11} - 9\bar{\varphi}_{10}^2\bar{\varphi}_{11} + 9\bar{\varphi}_{11}^3 + 4\bar{\varphi}_{11}\bar{\psi}_{21} \\ -\frac{4}{15}N_0N_1\bar{\varphi}_{11} + 5N_1\pi^3\bar{\psi}_{21} \end{pmatrix} \tag{4.22}$$

and

$$A = \begin{pmatrix} -N_2 + 2\pi^2 + 9\bar{\varphi}_{10}^2\pi^2 + 9\bar{\varphi}_{11}^2\pi^2 + 4\pi^2\bar{\psi}_{21} & 18\pi^2\bar{\varphi}_{10}\bar{\varphi}_{11} & 4\pi^2\bar{\varphi}_{10} \\ -18\pi^2\bar{\varphi}_{10}\bar{\varphi}_{11} & -N_2 + 2\pi^2 - 9\pi^2\bar{\varphi}_{10} + 27\pi^2\bar{\varphi}_{11}^2 4\pi^2\bar{\psi}_{21} & 0 \\ 5\pi^3N_1 & -\frac{36}{75}N_1\pi^2 & \frac{375}{75}N_0N_1 \end{pmatrix} \tag{4.23}$$

4.2.2 Discussion of Solutions

Solving for the stationary solutions by setting the derivatives equal to zero gives the equilibrium values for φ and ψ. We begin with the limit of $N_0 \to 0$ where no convection should exist. From Eqn. 4.16 we see that

$$\psi_{21} = \frac{4}{75\pi^3}N_0\varphi_{11}. \tag{4.24}$$

In the case of $N_0 \approx 0$ the stream mode ψ_{21} is negligibly small, since for all interesting cases φ_{kl} remains bounded between zero and one. Turning to Eqns. 4.14 and 4.15 we obviously have the trivial solutions ($\bar{\varphi}_{10}$,$\bar{\varphi}_{11}$) = (0,0) and can divide by one of the respective variables to obtain

$$0 = -\frac{N_2}{\pi^2} + 2 \ -\frac{3}{2}\bar{\varphi}_{10}^2 + 9\bar{\varphi}_{11}^2 + \frac{16}{75}N_0\varphi_{11} \tag{4.25}$$

$$0 = -\frac{N_2}{\pi^2} + 1 \ + 9\bar{\varphi}_{11}^2 - 9\bar{\varphi}_{10}^2 + \frac{16}{75}N_0\varphi_{11} \tag{4.26}$$

which has non-trivial solutions

$$\bar{\varphi}_{10} = \pm\sqrt{\frac{2}{15}} \text{ and } \bar{\varphi}_{11} = \pm\frac{\sqrt{5N_2 - 4\pi^2}}{\sqrt{35}\pi}. \tag{4.27}$$

We can then perform a bifurcation analysis, the diagram of which is presented in Fig.8. Of special interest is the case where coming from small N_2 and non-vanishing φ_{10} the stable solution has bifurcation which creates attracting focus. To analyse this behaviour we insert our solution for constant $\varphi \neq 0$ into the matrix A and compute the eigenvalues in dependence of the parameter N_2. We obtain

$$\lambda_1 = -\frac{24\pi^2}{5} \tag{4.28}$$

$$\lambda_2 = -\frac{1}{5}\left(5N_2 - 5\pi^2 - \sqrt{5}\sqrt{5N_2^2 - 30N_2\pi^2 + 21\pi^4}\right) \tag{4.29}$$

$$\lambda_3 = -\frac{1}{5}\left(5N_2 - 5\pi^2 + \sqrt{5}\sqrt{5N_2^2 - 30N_2\pi^2 + 21\pi^4}\right) \tag{4.30}$$

If we follow the real and complex part of the eigenvalues depicted in Fig. 9 we see that the discriminant of both eigenvalues equals zero if

$$N_{2,Hopf} = 3 - 2\sqrt{\frac{6}{5}}\pi^2 \approx 7.985 \tag{4.31}$$

From thereon two complex eigenvalues exist. Now it is also important to analyse if the Hopf bifurcation lies on a stable branch. Therefore, we check at when the real part of the eigenvalue λ_3 crosses zero. This happens at

$$N_2 = \frac{4\pi^2}{5} \approx 7.895 \tag{4.32}$$

where both eigenvalues are below zero so that the oscillations are decaying to the stable solution. However at $N_2 = \pi^2$ the solution branch becomes unstable again. From this we can deduce that there indeed is a critical N_2 from which on only the origin is a stable fix point. Furthermore, the stable solutions decay not solely to an unstable solution which ends at the x-axis, but are also continued via a bifurcation in φ_{10} and φ_{11}. This bifurcation exists even when we do not have the stream mode ψ_{11} present and vanishes at $N_2 = \pi^2$. To see if this rather exotic branch corresponds to physical reality, we take a closer look at the phase space to understand what is happening.

We start with $N_2 = 0$ and obtain the phase portrait found in Fig. 10. The nullclines cross at three different singular points. The first point for $\varphi_{11} = 0$ and negative $-\varphi_{10}$ is a stable knot with two distinctive negative eigenvalues; the point where $\varphi_{11} = \varphi_{10} = 0$ is an saddle point and possesses two distinctive but positive

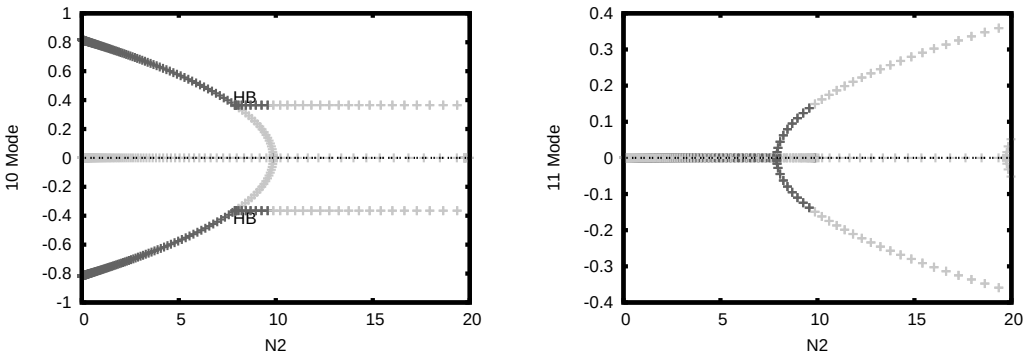

(a) φ_{10} (b) φ_{11}

Figure 8: Shown are the unstable solutions with the dashed line and the stable ones with a solid line. Here we have $N_0 = 0$. Looking from $N_2 = 0$ three solutions for φ_{10} exists, where the solutions starting from $N_2 \approx \pm 0.8$ are stable solutions that describes a physical solution. They loose stability when at the Hopf bifurcation a new stable solution with two complex eigenvalues emerges. This oscillatory solution on the other hand becomes again unstable in the vicinity of $N_2 \approx 10$.

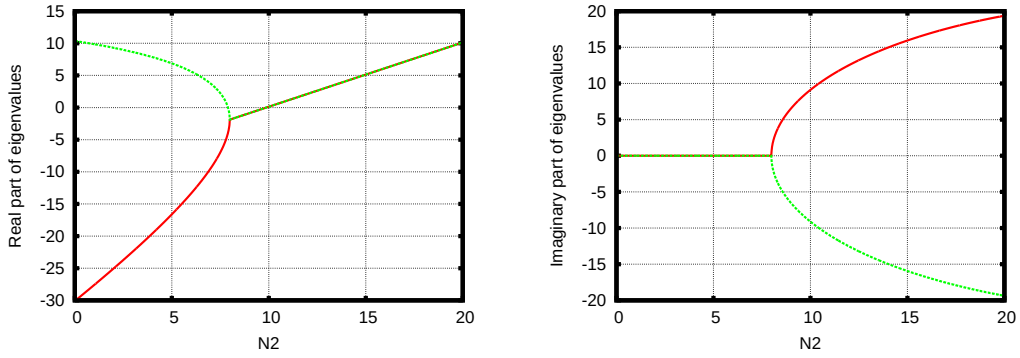

(a) Real part (b) Imaginary part

Figure 9: The real and imaginary parts of the eigenvalues of the matrix A for the non-trivial solution $\bar{\varphi}_{10} = \pm\sqrt{\frac{2}{15}}$ and $\bar{\varphi}_{11} = \pm\frac{\sqrt{5N_2 - 4\pi^2}}{\sqrt{35}\pi}$. The oscillatory solutions emerge where the pair of imaginary eigenvalues appears. It is stable as long as the real part is smaller than zero. The crossing to an unstable solution happens exactly at the point where the φ_{10} mode decays to possessing only an unstable solution.

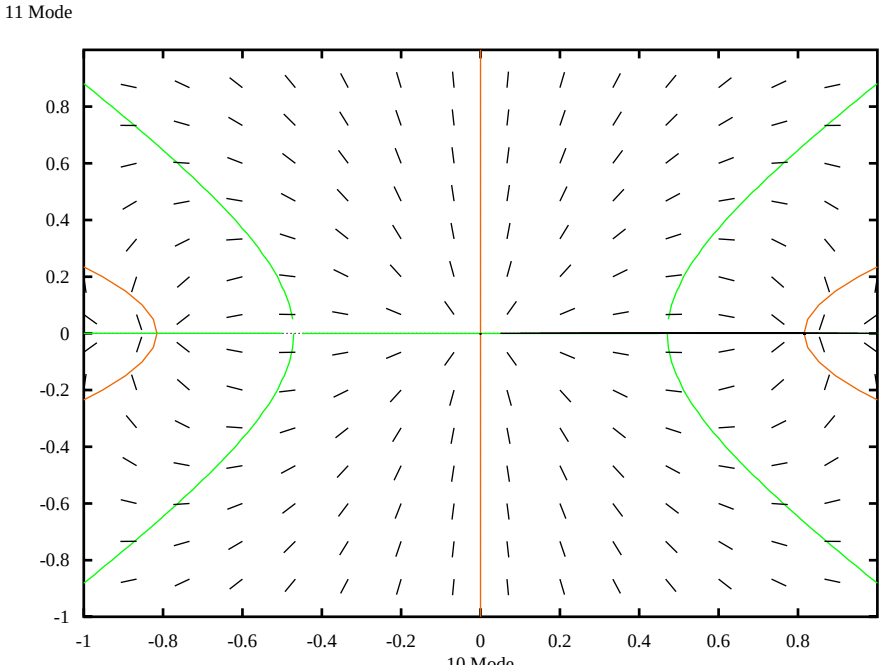

Figure 10: The nullclines for φ_{11} depicted as red line and φ_{10} depicted as green line intersect at singular points for $N_0 = 0$ and $N_2 = 10^{-5}$. The phase diagram is highly symmetric as has to be expected for the purely diffusional case, since the diffusion equation is invariant under rotations. There exist three points of special interest. The leftmost point were both nullclines intersect is a stable node as is the rightmost. The trivial solution $\varphi_{10} = \varphi_{11} = 0$ that is not physical is a repelling node.

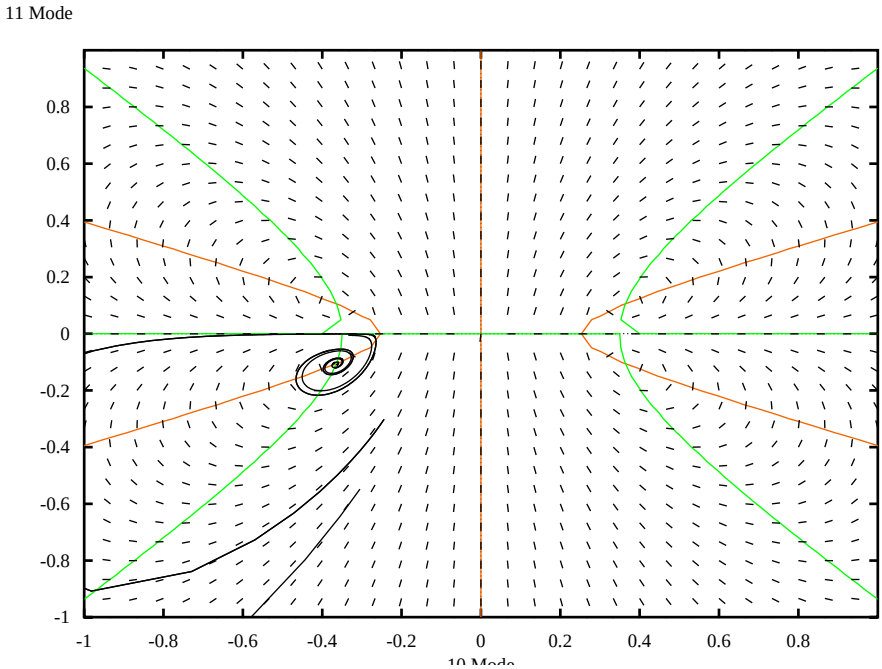

Figure 11: The nullclines for φ_{11} depicted as red line and φ_{10} depicted as green line intersect at singular points for $N_0 = 0$ and $N_2 = 9$. There are now 7 singular points. On the left part of the phase diagram there are two stable foci for one of which a spiralling trajectory is included. The attracting foci from Fig. 10 became repelling ones whereas the repelling node at the trivial solution remained unstable

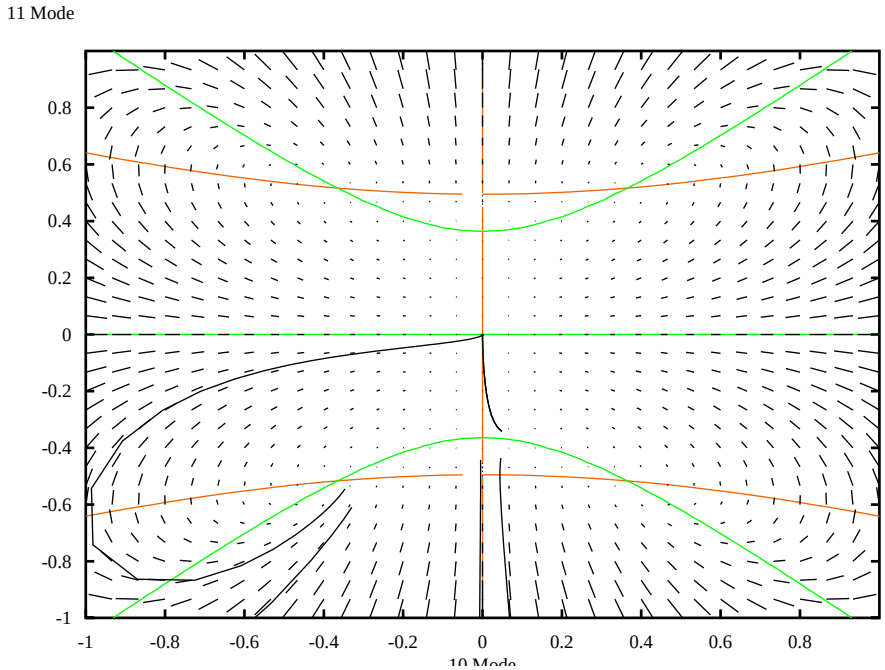

Figure 12: The nullclines for φ_{11} depicted as red line and φ_{10} depicted as green line intersect at singular points for $N_0 = 0$ and $N_2 = 100$. There are again 7 singular points. The stable foci lost their stability and now became repellent foci for which spiralling out trajectories are shown. The two nontrivial solutions for $\varphi_{11} = 0$ and $\varphi_{10} = \pm\bar{\varphi}_{10}$ turned into hyperbolic nodes with $\varphi_{10} = 0$ and $\varphi_{11} = \pm\bar{\varphi}_{11}$. Additionally the unstable source in the middle became a sink.

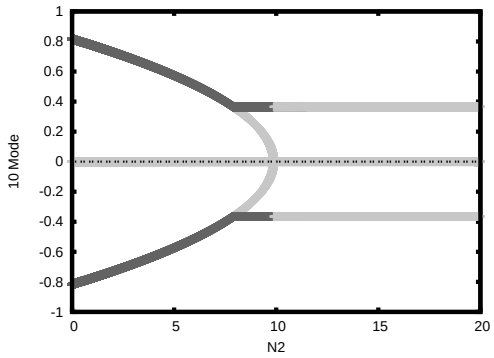

(a) φ_{10}

Figure 13: Shown are the unstable solutions with the dashed line and the stable ones with a solid line for the φ_{10} for $N_0 = 10^4$. The oscillatory solution also found for $N_0 = 0$ persists longer, because the ψ_{21} helps carrying away supersaturation.

eigenvalues. The third point with positive φ_{10} equals that of the first because of symmetry. Here, the fix point $\psi_{21} = \varphi_{11} = 0$ and $\varphi_{10} \neq 0$ represent the stable diffusive profiles

If N_2 is now increased to $N_2 = 9$ there are 7 singular points (cf. Fig. **??**). Since the phase space is highly symmetric we focus on the left side. Here two stable foci with complex conjugated complex parts and negative real part emerged from the stable knot that itself possesses now one positive and one negative real eigenvalue and became an unstable knot. The point for $\varphi_{10} = \varphi_{11} = 0$ still is unstable.

If N_2 is increased even further to $N_2 = 100$ we have still 7 singular points. The stable foci lost their stability and now have equal complex conjugated and positive real eigenvalues. The two nontrivial solutions for $\varphi_{11} = 0$ and $\varphi_{10} = \pm\bar{\varphi}_{10}$ remained hyperbolic points with $\varphi_{10} = 0$ and $\varphi_{11} = \pm\bar{\varphi}_{11}$. On the other hand the solution $\varphi_{10} = \varphi_{30}$ is now a stable attractor. This resembles a diffusively unstable system, since $\varphi_{ij} = 0$ for all modes would imply an infinite ϕ or zero ϕ_0. Both are unphysical or uninteresting solutions. Clearly, the 3 mode model does not faithfully describe the dynamics for such high heating rates.

These oscillations around the stable solutions are however problematic. In reality an oscillation in only the φ_{10} and φ_{11} mode would be highly unstable to gravity and can be considered an artifact in the three mode model.

We can now summarize the findings for the three mode model in a phase diagram of distinctive solutions in Fig 14. It can be divided into the following different areas: In the lower left region the heating rate and gravity is too weak to cause any insta-

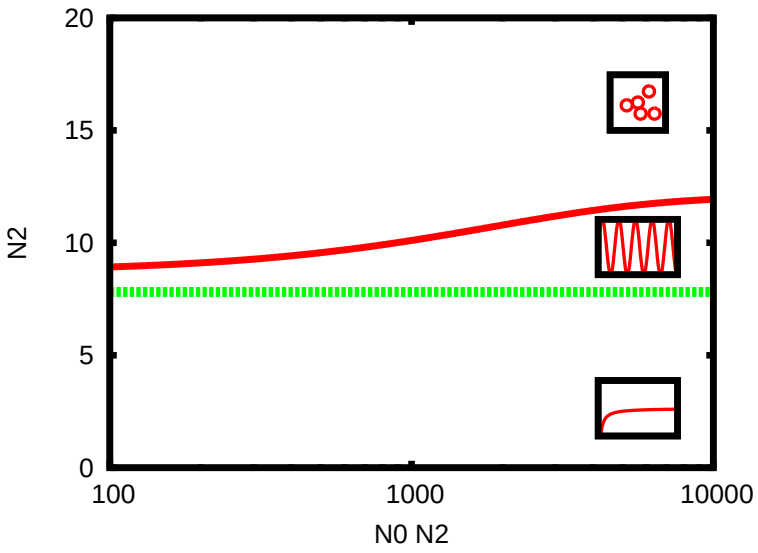

Figure 14: Plotted is the maximum combination of N_2 and N_0 for which stable, oscillatory solutions exist. Here, the onset of instability depends continuously on the parameter N_0 in such a way that an increase in strength of convection also increases the critical threshold $N_{2,cr}$. The reason for this is that, with convection, the supersaturation can be carried away more rapidly and therefore the system does not need to nucleate droplets or form a different kind of stable layering (e.g. a layering with $\frac{\Lambda}{3}$) in higher modes.

bilities, thus the system behaves in a stable way. If the rate of heating is increased while the gravitation stays constant, the system enters the region where the system shows oscillatory behaviour and then becomes diffusively unstable. What happens when the system enters this region can not be satisfyingly described with a 3 mode approximation, since addition of more modes will probably provide a decay channel for this solution.
Further, if the system is diffusively stable but N_0 is increased, e.g. by increasing the density difference between the fluids, the system should become convectively unstable and convection cells should start to form. This solution is missing in the 3 mode model. To get reasonable results we therefore have to incorporate additional modes.

4.3 The Five Mode Model

To investigate whether the model improves if more modes of supersaturation are taken into account we add the φ_{30} mode. At least this will allow for density inversion. Additionally, the φ_{31} must be incorporated, since it couples ψ_{21} to φ_{10}. These modes also allows us to compare our approach to the model of diffusive instability in[12] if we perform a stability analysis for stable φ_{10} and φ_{30}.
Computing the equations of motion yields:

$$\begin{aligned} 2\frac{\mathrm{d}\varphi_{10}}{\mathrm{d}t} = &-2\varphi_{10}N_2 + 2\varphi_{10}\pi^2 + 8\psi_{21}\varphi_{10}\pi^2 - 3\varphi_{10}^3\pi^2 + 18\varphi_{10}\varphi_{11}^2\pi^2 + \\ &3\varphi_{10}^2\varphi_{30}\pi^2 - 6\varphi_{11}^2\varphi_{30}\pi^2 - 6\varphi_{10}\varphi_{30}^2\pi^2 - 12\varphi_{10}\varphi_{11}\varphi_{31}\pi^2 + \\ &24\varphi_{11}\varphi_{30}\varphi_{31}\pi^2 + 12\varphi_{10}\varphi_{31}^2\pi^2 \end{aligned} \tag{4.33}$$

$$\begin{aligned} \frac{\mathrm{d}\varphi_{11}}{\mathrm{d}t} = &-(\varphi_{11}N_2) + 2\varphi_{11}\pi^2 + 4\psi_{21}\varphi_{11}\pi^2 + 9\varphi_{10}^2\varphi_{11}\pi^2 + 9\varphi_{11}^3\pi^2 + \\ &6\varphi_{10}\varphi_{11}\varphi_{30}\pi^2 - 6\varphi_{11}\varphi_{30}^2\pi^2 + 3\varphi_{10}^2\varphi_{31}\pi^2 - 9\varphi_{11}^2\varphi_{31}\pi^2 - \\ &12\varphi_{10}\varphi_{30}\varphi_{31}\pi^2 + 18\varphi_{11}\varphi_{31}^2\pi^2 \end{aligned} \tag{4.34}$$

$$\begin{aligned} 2\frac{\mathrm{d}\varphi_{30}}{\mathrm{d}t} = &-2\varphi_{30}N_2 + 9\varphi_{10}^3\pi^2 - 54\varphi_{10}\varphi_{11}^2\pi^2 + 18\varphi_{30}\pi^2 + 12\psi_{21}\varphi_{30}\pi^2 + \\ &54\varphi_{10}^2\varphi_{30}\pi^2 + 108\varphi_{11}^2\varphi_{30}\pi^2 - 27\varphi_{30}^3\pi^2 + \\ &216\varphi_{10}\varphi_{11}\varphi_{31}\pi^2 + 162\varphi_{30}\varphi_{31}^2\pi^2 \end{aligned} \tag{4.35}$$

$$\frac{\mathrm{d}\varphi_{31}}{\mathrm{d}t} = -(\varphi_{31}N_2) + 15\varphi_{10}^2\varphi_{11}\pi^2 - 15\varphi_{11}^3\pi^2 - 60\varphi_{10}\varphi_{11}\varphi_{30}\pi^2 + 10\varphi_{31}\pi^2 + 6\psi_{21}\varphi_{31}\pi^2 + 30\varphi_{10}^2\varphi_{31}\pi^2 + 90\varphi_{11}^2\varphi_{31}\pi^2 - 45\varphi_{30}^2\varphi_{31}\pi^2 + 45\varphi_{31}^3\pi^2 \tag{4.36}$$

$$75\frac{\mathrm{d}\psi_{21}}{\mathrm{d}t} = N_0N_1(36\varphi_{31} + 20\varphi_{11}) - 375N_1\pi^3\psi_{21} \tag{4.37}$$

To linearize it in the sense of [12] we make an ansatz of small variations around the stable diffusion profile

$$\varphi_{10} = \bar{\varphi}_{10} + \delta\varphi_{10} \tag{4.38}$$

$$\varphi_{30} = \bar{\varphi}_{30} + \delta\varphi_{30} \tag{4.39}$$

$$\varphi_{11} = \delta\varphi_{11} \tag{4.40}$$

$$\varphi_{31} = \delta\varphi_{31} \tag{4.41}$$

$$\psi_{21} = \delta\psi_{21} \tag{4.42}$$

$$\tag{4.43}$$

and define a vector of deviations as

$$\boldsymbol{\delta} = \begin{pmatrix} \delta\varphi_{10} \\ \delta\varphi_{30} \\ \delta\varphi_{11} \\ \delta\varphi_{31} \\ \delta\psi_{21} \end{pmatrix}. \tag{4.44}$$

With this we can write the system as seven linear ordinary differential equations in matrix form

$$\dot{\boldsymbol{\delta}} = A\boldsymbol{\delta} + \mathbf{b}, \tag{4.45}$$

where

$$\mathbf{b} = \begin{pmatrix} -N_2\bar{\varphi}_{10} + \frac{1}{2}\pi^2\left(-2\bar{\varphi}_{10} + 3\bar{\varphi}_{10}^3 - 3\bar{\varphi}_{10}^2\bar{\varphi}_{30} + 6\bar{\varphi}_{10}\bar{\varphi}_{30}\right) \\ -N_2\bar{\varphi}_{30} + \frac{3}{2}\pi^2\left(3\bar{\varphi}_{10}^3 + 6\bar{\varphi}_{30} - 18\bar{\varphi}_{10}^2\bar{\varphi}_{30} - 9\bar{\varphi}_{30}^3\right) \\ 0 \\ 0 \\ 0 \end{pmatrix} \tag{4.46}$$

and

$$A = \begin{pmatrix} -N_2 - \frac{1}{2}(-2 + 9\bar{\varphi}_{10}^2 - 6\bar{\varphi}_{10}\bar{\varphi}_{30} + 6\bar{\varphi}_{30}^2) & \frac{3}{2}\pi^2(\bar{\varphi}_{10} - 4\bar{\varphi}_{30}) & 0 & 0 & 4\pi^2\bar{\varphi}_{10} \\ \frac{27}{2}\pi^2\bar{\varphi}_{10}^2 - 4\bar{\varphi}_{10}\bar{\varphi}_{30} & -N_2 - \frac{9}{2}\pi^2(-2 + 6\bar{\varphi}_{10}^2 + 9\bar{\varphi}_{30}^2) & 0 & 0 & 6\pi^2\bar{\varphi}_{30} \\ 0 & 0 & (-N_2 - \pi^2(-2 + 9\bar{\varphi}_{10}^2 - 6\bar{\varphi}_{10}\bar{\varphi}_{30} + 6\bar{\varphi}_{30}^2)) & 3\pi^2(\bar{\varphi}_{10}^2 - 4\bar{\varphi}_{30}) & 0 \\ 0 & 0 & -15\pi^2(\bar{\varphi}_{10}^2 - 4\bar{\varphi}_{30}\bar{\varphi}_{10}) & N_2 + 5\pi^2(-2 + 6\bar{\varphi}_{10}^2 + 9\bar{\varphi}_{30}^2) & 0 \\ 0 & 0 & \frac{375}{75}N_0N_1 & \frac{20}{75}N_0N_1 & -\frac{36}{75}N_1\pi^2 \end{pmatrix} \tag{4.47}$$

Thereby we obtained the same **b** aside from a numerical factor π^2 as in [12] for a one-dimensional model without stream function.

However, since the present set of equations hard to solve analytically and we thus have to use numerical means in any case, we can also perform a bifurcation analysis of the full system, allowing also for stable φ_{11},φ_{31} and ψ_{21} solutions. The bifurcation diagram in Fig. 15 resembles the one from the three mode model in the sense that the φ_{10} solutions that appeared for small N_2 as stable solutions are still part of the diagram. However, these solutions are now unstable and are absorbed by stable pairs of φ_{10} and φ_{30}. This is reasonable, since one would expect that a vertical 2 mode approximation will be a much better description of a stable profile than one based on only one mode. Also, there are no more stable φ_{11} and no φ_{31} solutions. This as well depicts reality far better, since the layering with e.g. φ_{11} is susceptible to small deviations and should loose stability if nudged slightly. The exotic oscillations in only $\varphi_{10}, \varphi_{11}$ without stream function do not exist any longer and there are new asymptotically-stable solutions for ψ_{21}, that still oscillate and help to carry away supersaturation, but do not decay to ψ_{21}. These solutions emerge from the stable φ_{10} solutions near $N_2 \approx 4.8$. A sample plot for $N_2 = 10$, $N_0 = 10^4$ can be found in Fig. 16. Now since we have a stable convection cell, we can look for the onset of stable ψ_{21} solution in dependence of N_0 and N_2. Also we can look at how long there exists oscillatory solutions in dependence of N_2 and N_0.

The corresponding phase diagram can be found in Fig 17. The oscillatory solutions behave much like they did for the three mode model, with the exception that now, since φ_{11} and φ_{31} are unstable, no oscillations in the limit of vanishing N_0 exists. They exist for larger N_2 if the convection can act stronger with larger N_0.

The threshold for the onset of convective resembles the one found in section 3. They are compared in Fig. 18 and they converge for small N_2 as is expected. In conclusion,

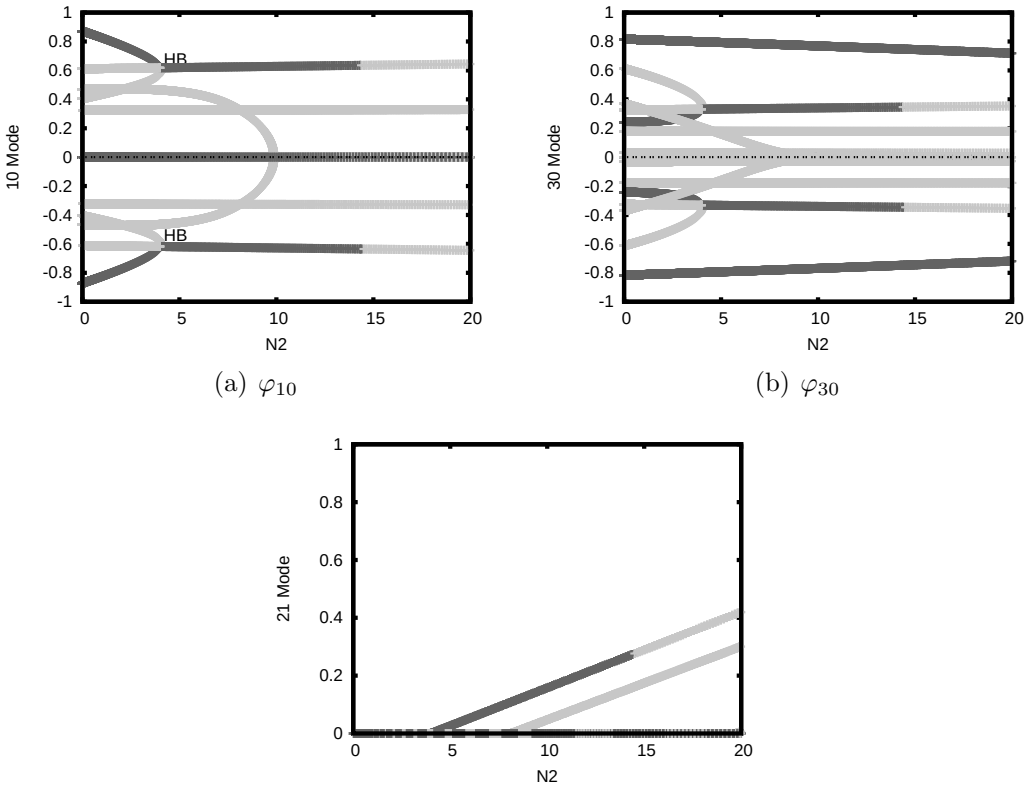

(a) φ_{10} (b) φ_{30}

(c) ψ_{21}

Figure 15: Shown are the unstable solutions with the dashed line and the stable ones with a solid line for $N_0 = 10^4$.

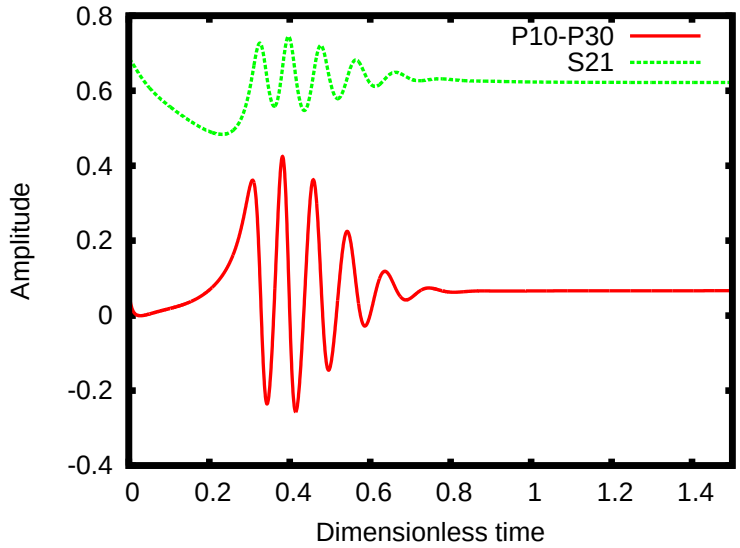

Figure 16: After a transient the maximum $\phi_{10} - \phi_{30}$ shows oscillations that decay into the stable solutions. It is aided by the stream mode ψ_{21} which also tends to a stable solution.

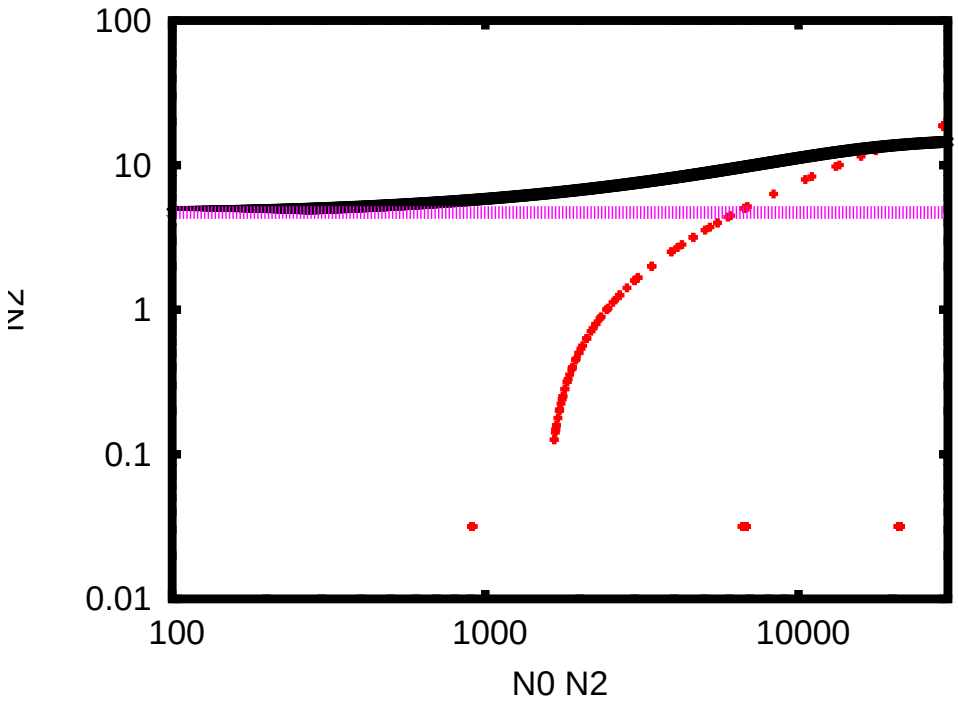

Figure 17: The phase diagram consists of mainly five different regimes in which solutions differ topologically. In the lower left part both the heating rate and the gravitation is weak enough to keep the system stable. If the heating rate is increased the system can enter the upper left part in which it loses stability to nucleation. If the gravity parameter N_0 is increased the system may enter the lower right side in which convection cells form and the system becomes convectively unstable. If both, gravity and heating rate are chosen in a suitable manner, the system may enter a oscillatory region in the centre or the upper right hand side in which the solutions oscillate around a stable diffusive solution.

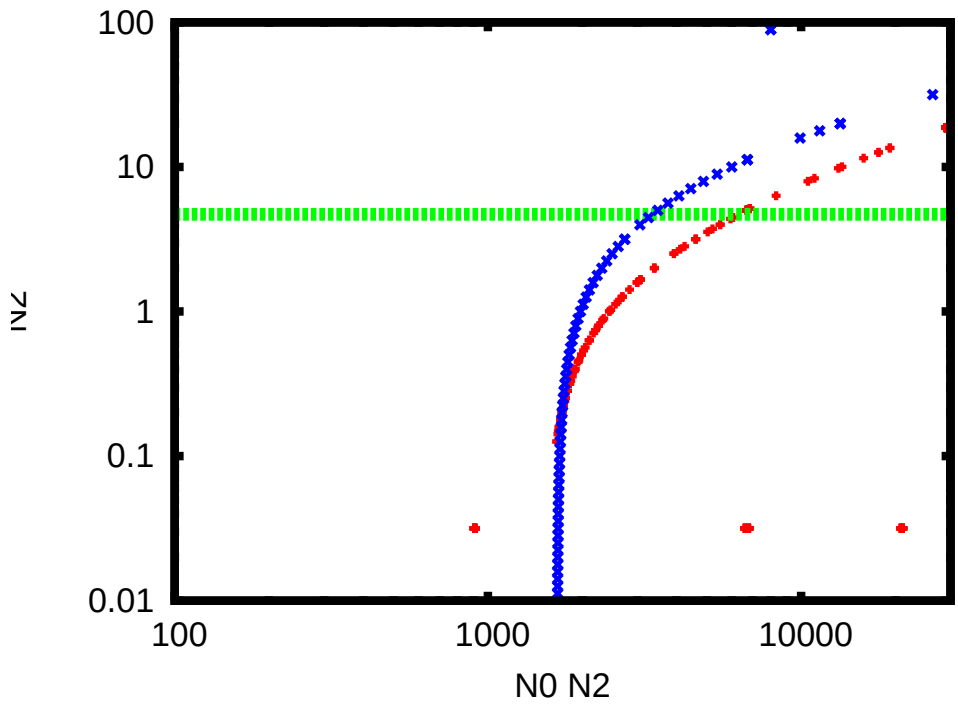

Figure 18: The red line gives the threshold for a stable convection cell in the Landau five mode model. The blue line gives the reference threshold computing in section 3. The lack of coverage for the red line approaching $N_2 = 0$ is due to numeric artifacts when the slope becomes too large for reasonable computing times. Of particular importance is that they resemble each other in the limit of $N_2 \to 0$.

we can say that the 5 mode model provides a fair picture of the behaviour of the demixing. It would be highly desirable, however, to see in how far these results keep changing when more modes are added.

5 Discussion and Conclusion

5.1 Summary

In this work we have explored the emergence of convective instabilities in the demixing of binary fluids being subjected to a small temperature drift. It shares certain aspects with the Rayleigh-Benard-Problem but it appears to have its own, very rich set of bifurcations for larger heating rates..
We considered a symmetric binary fluid whose thermodynamics is governed by a free energy that was chosen according to a expansion in the critical parameter, the composition ϕ, as a polynomial of degree four in ϕ. This corresponds to the well known ϕ^4-ansatz of Landau to describe demixing. The composition is advected by a flow described by the Navier-Stokes-Equations in Boussinesq approximation. The two main parameters which govern the dynamics are the heating rate N_2 and the strength of gravitation N_0.
First, we approximated the diffusion equation for small values of N_2 in a Taylor expansion and computed the critical number of N_0N_2 for the onset of convection cells. We provided them furthermore in dependence of the heating rate N_2 and thus obtained one piece of a phase diagram of instabilities of the system
We then proceeded and used a full Landau-ϕ^4-ansatz for computing the onset of diffusive instability in a Galerkin expansion. For some values of N_2 there exist oscillatory solutions in the five mode model with a non-vanishing convection mode whose solutions remain stable for larger N_2 when N_0 is increased because the convection helps carrying away supersaturation. We provided the critical values for the onset of convection based on an explicit expression for the steady-state concentration field, which holds for $N_2 \ll 1$, and is a five mode model where the composition is expanded to 2nd order in a Fourier series. The latter model also allowed us to explore how the stable diffusive profile becomes unstable with increasing heating rate. In that case a limit cycle is born where convection periodically kicks in to remove the supersaturation.

5.2 Discussion

The model makes a number of assumptions which might be relaxed in forthcoming work:

1. The diffusion equation is based on a Landau-ϕ^4-ansatz. It is derived as a mean-field theory and one has to be careful to choose the length scale of smallest correlation length right and not run into any problems of renormalisation [7]. In our case this is not a problem since we do not directly look at the behaviour at the critical point.

2. The analysis neglects the effect of surface tension. With the help of AUTO we performed additional numerical tests to verify that the described scenarios are robust with respect to explicitly implementing a surface tension. Nevertheless, the surface tension can also exhibit further tensorial behaviour and is certainly an interesting point of investigation.

3. We assume the system to be isothermal. This can be problematic if the heating rate ξ which leads to an exponentially increasing temperature ramp is chosen too high in a long experimental run. We know that even small gradients in temperature can lead to convection rolls (see e.g. [1]). However not too far from the critical point the ramp rate is still slow. This means that the time evolution may well be changed by a double diffusive system and may also exhibit instabilities (analysed by [11]) but it still remains valid near the critical point T_c.

4. Another approximation lies in the Boussinesq model for the Navier-Stokes-Equations together with the continuity condition. Here, the buoyant up-drift driven by a change in density contradicts the assumption that $\nabla.\rho = 0$. This model however has been shown to provide faithful results and especially Lücke et al. discussed when the Boussinesq approximation looses its validity [10],[13].

5. In the first part we constricted our analysis to a two dimensional system. Also this will in general not alter the description of convection, it may alter the results obtained by the mean field approximation, for these may depend on dimension [3]. This should turn out to be a negligible problem, since close to the threshold cellular convection patterns can be represented as a superposition of individual cells with different orientation of the axes [6].

6. The Fourier expansion of the concentration field can not faithfully represent bubbles. Hence, we are not able to investigate bubble solutions. This is inherent to the method we chose. There are genuine attempts to tackle the bubble problem (cf. work by Izabella Benczik [**?**] and Tobias Lapp)

5.3 Outlook

The beauty of the present model lies in the fact that it describes interesting and relevant features of demixing in terms of only very few model parameters. As outlined above, it can serve as a starting point of more detailed studies to discover even more generic properties of the phase separation.
The road ahead is the comparison with experiment and different numeric approaches to gain further insight into when the different approaches converge and the careful analysis of the physics we learn to understand along the way.

Acknowledgements

I would like to thank everyone, who supported me with creating this thesis, without your support this work would not have been possible. Special thanks is provided for my supervisor Prof. Jürgen Vollmer, who helped me with all the problems that crossed my way and did not fear to tackle nasty equations at all times of the day and is an inspiring and enthusiastic teacher even at the odd hours and for Prof. Ulrich Parlitz who willingly accepted to be the second referee. Furthemore I have to thank all the inhabitants of the ivory tower and our group, especially Tobi, Heiko, Artur, Johannes, Ariane, Izabella, Mitja, Daniel, Bernhard, Ilenia, Christian and Martin. Also, I would like to specially thank Frank Dettenrieder who lay the foundation for this work with his diploma thesis.

Appendix

A Phase Transitions

According to the Ehrenfest classification phase transitions can be categorized dependent on the discontinouities of the free energy of a system. An n'th order phase transition orginates from a discontinouity in the n'th derivative of the free energy F or a divergence in one of the parameters F dependens on. Additionally there are critical or continous phase transitions. In both cases the free energy can be calculated via statistical mechanics and the Gibbs relation

$$e^{\frac{F}{k_b T}} = \mathrm{Tr} e^{-\frac{H}{k_b T}}. \tag{A.1}$$

In theory a phase diagram can be calculated in dependence of the critical[7] parameter just by considering an optimal Hamiltonian and thus being able to just calculate the free energy. This, however, is not a trivial problem.
If we want to tackle it, wie look at the observable $\hat{\phi}$ that corresponds to our critical parameter ϕ[8] that may depend on position and have to average over the system size. Also we have to give a free energy F.

A.1 Mean Field Approach

Our aim is to describe the critical parameter ϕ in form of a global observable. For this we use a mean field approximation. This means that each particle of the fluid interacts with the average composition of the system or in other words, that each degree of freedom interacts with the average of the ramainder of degrees of freedom. The observable $\hat{\phi}$ may also depend on position so that it must be averaged over some length l which is well in between the system size (otherwise the observable would not be very useful) and the intermolecular forces (so that fluctuations on this scale are evened out). This means we have to find out what length l is optimal and also if there is a good way to compute the free energy of our system.
Luckily, Landau proposed a theory that there exists a Landau free energy density

[7] We call a parameter critical if the system has a large susceptibility to little changes in it near a phase transition or some other order to disorder transition. This can also be viewd in the light of self-simalirity in correlation. A slight fluctuation in a critical parameter near the transition will induce a cascade of system changes along a multitude of length scales thereby exhibiting a correlation among those.

[8] In a binary mixture ϕ is simply a measure of concentration of one of the phases.

that depends on the coupling constants that describe the strength of particle interaction and on some critical parameter. This Landau free energy should have the properties that it respects the symmetries of the system, can be exactly expressed as a polynomial series and that this series is finite[9]
In the case of our binary fluid the Landau free energy density functional should be symmetric in ϕ, have a low order, so that it captures the relavant physics of phase separation but facilitates calculations and contain a simple coupling term. In the case of demixing a order of 4 has appeared to be a good choice so that we as well choose

$$F_0[\phi(\mathbf{r},t)] = \int \left(\frac{b}{4}\phi^4 - \frac{a}{2}\phi^2 + f(\phi,K) \right) \mathrm{dV}, \tag{A.2}$$

where f depends on ϕ and a coupling constant. Physically this coupling represents the penalty for crossing adjacent cells in the averaging procedure and may be interpreted as surface tension. Let us denote two adjacent blocks with $\phi(\mathbf{r}$ and $\phi(\mathbf{r}+\boldsymbol{\delta})$, then the simplest coupling between them is achieved by

$$\left(\frac{\phi(\mathbf{r}) - \phi(\mathbf{r}+\boldsymbol{\delta})}{\lambda^2} \right)^2 \tag{A.3}$$

where λ is the correlation length l over that we can also average. In the continuum limit this becomes a gradient and therefore

$$F_0[\phi(\mathbf{r},t)] = \int \left(\frac{b}{4}\phi^4 - \frac{a}{2}\phi^2 + \frac{K}{2}(\nabla\phi)^2 \right) \mathrm{dV} \tag{A.4}$$

. At this point we still have to show that this Landau free energy density corresponds in some limit to the actual free energy, futhermore we need to compute the correlation length. We start with the first.
In thermodynamic equilibrium the probability distribution for the critical parameter is given by

$$P[\phi] = \frac{e^{-\beta F[\phi])}}{Z} \tag{A.5}$$

[9]If a series expansion is finite, the taylor series contains only a finite number of derivatives and therefore incorporates only behaviour in some neighbourhood. To include global behaviour it would have to be expressed with derivatives up to ∞

where Z is the partition function. This partition function depends on all possible values for the critical parameter, that means we have to evaluate a path integral

$$Z = \int \mathfrak{D}\phi e^{-\beta F[\phi])}. \tag{A.6}$$

Furthermore in a coarse grained system where we have different blocks of ϕ we actually integrate

$$Z_i = \int \mathfrak{D}\phi e^{-\beta F[\phi(\mathbf{r}_i])}. \tag{A.7}$$

This is necessary for that it is now possible to go back with

$$F = -k_b T \ln Z \tag{A.8}$$

this free energy has the same properties as a normal free energy, the most important being for now that it is convex. Since if we know that F is convex, we can show that it is minimized by a statistical operator. Then we have shown all the porperties for the usual free energy and may use it without hindthoughts.
To show this, consider a statistical operator $\hat{\phi}$[10] and $\hat{\phi}'$. Then

$$\mathrm{Tr}\,\hat{\phi}'(\ln\hat{\phi} - \ln\hat{\phi}') \leq 0 \tag{A.9}$$

We can now define a free energy as a density functional acting on the observable

$$F[\hat{\phi}'] = \mathrm{Tr}\,\hat{\phi}'(H + k_b T \ln\hat{\phi}') \tag{A.10}$$

If we then find the correspondence to the inner energy in the first term and to the scaled entropy in the second term on the RHS, we can obtain the partition function

$$Z = \mathrm{Tr}\, e^{-\beta H} \tag{A.11}$$

so that the free energy becomes

$$F[\hat{\phi}'] = \mathrm{Tr}\hat{\phi}'[H - k_b T(\ln Z + \beta H)] \tag{A.12}$$

which equals

$$F[\hat{\phi}'] = -k_b T \ln Z = F \tag{A.13}$$

[10] In general this can be an arbitrary observable but we will stick with the notation for a relavant variable for this work

and thus equals the thermodynamic free energy of the system. From the inequality A.9 we can deduce that

$$F[\hat{\phi}] \leq F[\hat{\phi}']. \tag{A.14}$$

This means that in the density functional free energy takes a minimum value and then equals the thermodynamic free energy. Therefore if we know a free energy in dependence of $\hat{\phi}$ we now know how to relaxate the system to equilibrium.

References

[1] Chandrasekhar, S., 1981, *Hydrodynamic and Hydromagnetic Stability* (Dover Publications).

[2] D. Vollmer, A. W., J. Vollmer, 2002, Phys. Chem. Chem. Phys **4**, 1380.

[3] Dieterich, W., 2000, *Theorie der Phasenübergänge*, Technical Report, Universität Konstanz.

[4] Ehrenfest, 1933, Verhandlungen der Koninklijke Akademie von Wetenschappen **36**, 153.

[5] Feynman, R. P., 1998, *Statistical Mechanics* (Advanced Book Classics).

[6] Gespard, P., 1998, *Chaos, Scattering and Statistical Mechanics* (Cambridge University Press).

[7] Goldenfeld, N., 1992, *Lectures on Phase Transitions and the Renormalization Group*, Frontiers In Physics (Westview).

[8] Hagen Kleinert, V. S.-F., 2001, *Critical Properties of Phi4-Theories* (World Scientific).

[9] Hohenberg, P. C., and B. I. Halperin, 1977, Rev. Mod. Phys , 435.

[10] Lücke, M., 1987, Phys. Rev A **36**, 3505.

[11] Schöpf, W., 1993, Physical Review E **47**.

[12] Vollmer, J., 2008, AIP **129**(16).

[13] Vorobev, A., 2010, Arxiv.org .

Erklärung nach §13(8) der Prüfungsordnung für den Bachelor-Studiengang Physik und den Master-Studiengang Physik an der Universität Göttingen:

Hiermit erkläre ich, dass ich diese Abschlussarbeit selbständig verfasst habe, keine anderen als die angegebenen Quellen und Hilfsmittel benutzt habe und alle Stellen, die wörtlich oder sinngemäß aus veröffentlichten Schriften entnommen wurden, als solche kenntlich gemacht habe.
Darüberhinaus erkläre ich, dass diese Abschlussarbeit nicht, auch nicht auszugsweise, im Rahmen einer nichtbestandenen Prüfung an dieser oder einer anderen Hochschule eingereicht wurde.

Göttingen, den 24. Januar 2011

(Jan-Hendrik Trösemeier)